In Vivo and *In Vitro* Neurotoxicity of the Human Prion Protein (PrP) Fragment P118–135 Independently of PrP Expression

Joëlle Chabry,[1] Christiane Ratsimanohatra,[2]* Isabelle Sponne,[3]* Pierre-Paul Elena,[2] Jean-Pierre Vincent,[1] and Thierry Pillot[3]

[1]Institut de Pharmacologie Moléculaire et Cellulaire, Unité Mixte de Recherche 6097, Centre National de la Recherche Scientifique, 06560 Valbonne, France, [2]Iris Pharma, Les Nertières, 06610 La Gaude, France, and [3]Institut National de la Santé et de la Recherche Médicale, Université de Nancy I, 54505 Vandœuvre-les-Nancy, France

We recently demonstrated that the 118–135 putative transmembrane domain of prion protein (PrP) exhibited membrane fusogenic properties and induced apoptotic neuronal cell death of rat cortical neurons, independently of its aggregation state. The aim of the present study was to analyze the *in vivo* neurotoxicity of the prion fragment P118–135 and to evaluate the potential role of the physiological isoform of PrP in the P118–135-induced cell death. Here, we demonstrate that the nonfibrillar P118–135 is cytotoxic to retinal neurons *in vivo* as monitored by intravitreal inoculation and recording of the electrical activity of retina and tissue examination. Moreover, knock-out PrP gene mice exhibit similar sensitivity to the nonfibrillar P118–135-induced cell death and electrical perturbations, strongly suggesting that cell death occurs independently of PrP expression. Interestingly, a variant nonfusogenic P118–135 peptide (termed P118–135θ) had no effects on *in vivo* neuronal viability, suggesting that the P118–135-induced cell death is mediated by its membrane destabilizing properties. These data have further been confirmed *in vitro*. We show that the fusogenic peptide P118–135 induces death of cultured neurons from both wild-type and knock-out PrP gene mice via an apoptotic-mediated pathway, involving early caspase activation and DNA fragmentation. Altogether these results emphasize the neurotoxicity of the fusogenic nonfibrillar PrP transmembrane domain and indicate that fibril formation and PrP expression are not obligatory requirements for neuronal cell death. The use of synthetic prion peptides could provide insights into the understanding of neuronal loss mechanisms that take place during the development of the various types of spongiform encephalopathies.

Key words: **prion peptide; retina; apoptosis; *in vivo;* caspase activities; electroretinogram**

Introduction

Transmissible spongiform encephalopathies (TSE) are fatal neurological disorders including Creutzfeldt-Jakob disease and Gerstmann-Straüssler-Scheinker syndrome (GSS) in humans, scrapie in sheep and goats, and bovine spongiform encephalopathy in cattle. Common pathological characteristics of TSE are, among others, vacuolization of the neuropils, severe gliosis, and degeneration of neurons (Fraser, 1993). The accumulation in the brain of scrapie-infected animals of large aggregates of a pathological isoform [prion protein (PrP)sc, also called PrP-res] of the normal cellular prion protein (PrPc or PrP-sen) is usually observed (Kretzschmar et al., 1986; Locht et al., 1986). Although PrP-res has been proposed to be responsible for both transmission and pathogenicity of TSEs, the occurrence of natural and experimental TSEs in the absence of PrP-res accumulation demonstrates that the aggregation step is not an obligatory requirement for neurodegeneration. Moreover, PrP-res preparation injected intracerebrally into PrP gene knock-out mice ($PrP^{0/0}$) fails to cause disease and to provoke neural damages. These observations raise the possibility that PrP-res is not directly toxic by itself and support the idea that the development of TSEs requires the presence of both prion protein isoforms, PrP-res and PrP-sen.

Other aspects of PrP-sen biosynthesis such as aberrant subcellular location and topology may greatly influence the pathogenicity. Cell-free translation system studies (Hay et al., 1987; Lopez et al., 1990) demonstrated that PrP could be found in several topologic forms, including a transmembrane spanning domain isoform (termed ^{Ctm}PrP). Mice carrying a mutated PrP gene that favors markedly the synthesis of ^{Ctm}PrP show spontaneous neurodegeneration without detectable PrP-res accumulation (Hegde et al., 1998, 1999). The extent of neurodegeneration correlates with the amount of ^{Ctm}PrP, suggesting that ^{Ctm}PrP is directly responsible for neuronal cell death. Brains of GSS-affected patients bearing the A117V PrP mutation contain higher levels of ^{Ctm}PrP as compared with other human TSE-affected brains, but they fail to present PrP-res deposits. It is likely that the A117V PrP mutation may influence ^{Ctm}PrP accumulation, resulting in the

Received Aug. 22, 2002; revised Oct. 18, 2002; accepted Oct. 22, 2002.

This work was supported in part by French Government grants from the Action Concertée Incitive Jeunes Chercheurs (2000), the Action Thématique Concertée-Prions (Institut National de la Santé et de la Recherche Médicale), and the Groupement d'Intèrêt Scientifique: infections à prions (2001). We are grateful to Dr. Charles Weissmann for providing the $PrP^{0/0}$ mice. We thank Jean-Daniel Barde for animal care, Roxane Pichot for technical assistance, and Nicole Zsürger for help with the preparation of the figures. We thank Drs. Nathalie Daude and Jean-Louis Nahon for critical reading of this manuscript.

*C.R. and I.S. contributed equally to this work.

Correspondence should be addressed to Joëlle Chabry, Institut de Pharmacologie Moléculaire et Cellulaire, Unité Mixte de Recherche 6097, Centre National de la Recherche Scientifique, 660 Route des Lucioles, 06560 Valbonne, France. E-mail: chabry@ipmc.cnrs.fr.

 0270-6474/03/230462-08$15.00/0

neuropathological changes observed in GSS-affected brain; however, the molecular events triggered by the nonaggregated ^{Ctm}PrP and leading to neurodegeneration remain unknown.

The ^{Ctm}PrP isoform spans the endoplasmic reticulum membrane at residues 113–135 with its N-terminus domain facing the cytosolic compartment (Hegde et al., 1998). We and others have used the putative transmembrane domain of ^{Ctm}PrP, e.g., amino acids 118–135, to model and characterize apoptotic neuronal death associated with topological variants of PrP-sen (Haik et al., 2000; Pillot et al., 2000). In contrast to the PrP fragment 106–126, which required both fibrillation and the presence of PrP-sen to exert its neurotoxicity (Brown et al., 1996), we demonstrated that the nonfibrillar peptide P118–135 induced apoptosis of cortical neurons (Pillot et al., 2000), an effect mediated in part by its membrane perturbation properties (Pillot et al., 1997) (for review, see Brasseur et al., 1997).

In the present study, we address the question of the *in vivo* neurotoxicity of the nonfibrillar prion peptide P118–135 on both wild-type and PrP-devoid mice. We demonstrate that direct injection of soluble P118–135 into mouse eyes induces cell death of retinal neurons via an apoptotic pathway independent of PrP expression. Moreover, primary cultures of neurons from brains of both wild-type and PrP gene knock-out mice were treated with the fusogenic P118–135 peptide, and morphological and biochemical hallmarks of apoptotic cell death were investigated.

Materials and Methods

Materials. The caspase substrates Asp-Glu-Val-Asp-*p*-nitroanilide (DEVD-pNA; caspase-3 substrate), Tyr-Val-Ala-Asp-*p*-nitroanilide (YVAD-pNA; caspase-1 substrate), IEPD-AMC (caspase-8 substrate), and LEHD-AMC (caspase-9 substrate) were purchased from Bachem. Serum-free medium Neurobasal, N2 supplement, and penicillin–streptomycin mixture were from Invitrogen (Gaithersburg, MD). All other reagents were of highly purified grade from Sigma (St. Louis, MO).

Peptides. The human sequences of the prion protein fragments P118–135 (AGAVVGGLGGYMLGSAMS, fusogenic) and P118–135θ (AGGVVGGLGGYMLASAMS, nonfusogenic) were synthesized as described previously (Pillot et al., 1996, 1997). These peptides differ at two positions (underlined). Peptides were dissolved in PBS at a concentration of 1 mM, distributed into 20 μl aliquots, and stored at −20°C until use. Under these conditions, the peptides remain soluble (Pillot et al., 2000). To obtain amyloid fibrils, the P118–135 peptide should be incubated at a 1 mM concentration for 72 hr at room temperature (Pillot et al., 1997, 2000). The human sequence of the prion protein fragment (P106–126, KTNMKHMAGAAAAGAVVGGLG) was purchased from Bachem.

Intravitreal injection. Adult male C57-black wild-type or PrP$^{0/0}$ mice [named Zurich I; Büeler et al. (1992)] (10–12 weeks old) were anesthetized with an intraperitoneal injection of 60 mg/kg sodium pentobarbital. Injections (1 μl) of peptides or vehicle (PBS) were done unilaterally with a 33 gauge needle introduced into the posterior chamber on the upper pole of the eye directed toward the center of the vitreous. The injections were performed slowly to allow a better diffusion of the peptide and to avoid any ocular hypertension. For negative controls, mice were injected in the same conditions with 1 μl of vehicle (PBS). No significant differences in the a- and b-wave values were observed between the noninjected eyes and the eyes injected with 1 μl of PBS. At least three animals were used for each experimental condition.

Electroretinograms. Full-field electroretinogram (ERG) responses were obtained with overnight dark-adapted mice prepared under dim red light before recording. The pupils of anesthetized mice were dilated with a drop of 0.5% Mydriaticum. A silver chloride ring-recording electrode was placed on the cornea, and the reference electrode, with a silver–silver chloride tip, was introduced into the mouth. Light stimulus (15 msec) was provided by a single flash placed 0.25 m in front of the animal. The ERGs were recorded using the EPIC-2000 (LKC Technologies) visual electroretinogram test system and then stored and analyzed. Amplitude of the a-wave was measured from the baseline to the bottom of the a-wave; b-wave amplitude was measured from the bottom of the a-wave to the peak of the b-wave. The averaged responses represent the mean of two white flashes delivered 2 min apart. Electroretinograms were recorded before peptide treatments and then 1 and 7 d after injection. At the end of the ERG recording experiments, the histology and the *in situ* terminal deoxynucleotidyl transferase-mediated biotinylated UTP nick end labeling (TUNEL) method were performed as described previously (Ettaiche et al., 2000). Briefly, mice were euthanized with an overdose of sodium pentobarbital 1 and 7 d after intravitreal injections. The eyes were enucleated and fixed in ice-cold 4% paraformaldehyde in PBS for 24 hr and then cryoprotected overnight in PBS containing 20% sucrose. The eyes were then embedded in O.C.T. compound (Tissue-Tek, SAKURA, Tokyo, Japan), and frozen sections (10 μm) were cut on a cryostat (Leica, Nussloch, Germany). *In situ* cell death detection was performed on 1 d treated eyes, following the manufacturer's recommendations (Boehringer Mannheim, Mannheim, Germany) and then revealed using a 3,3′-diaminobenzidine (DAB) substrate kit (Vector Laboratories, Burlingame, CA). Morphological and histological observations of 7 d treated retinas were done on stained sections with 1% cresyl violet and then processed for detailed examination by light microscopy.

Cell culture. Cortical neurons from embryonic day (E) 13–14 C57-black wild-type or PrP$^{0/0}$ mice were prepared as described previously (Chabry et al., 1990) with minors modifications. Briefly, cells were dissociated mechanically with a Pasteur pipette in a chemically defined Neurobasal medium containing N2 supplement and penicillin–streptomycin. Dissociated cells were then plated at a density of 3×10^6 cells in 35 mm tissue plastic dishes (or 5×10^4 cells in 96-well tissue plates) precoated with polylysine (10 μg/ml) and grown at 37°C in humidified atmosphere of 5% CO_2, 95% air. After 3 d *in vitro*, cells were incubated with cytosine arabinoside (50 μM), an inhibitor of mitosis, to prevent glial cell proliferation. For the different experiments described below, neurons were used after 4–5 d of *in vitro* culture.

Cytotoxicity assay. Ninety-six-well tissue-plated neurons were treated in the absence or presence of various concentrations of indicated peptides for different periods of time. The neurotoxicity of the peptides was assessed quantitatively by the (3-(4,5-dimethylthiazol-2-yl)-5-(3-carboxymethoxyphenyl)-2-(4-sulfophenyl)-2H tetra-zolium (MTS) (Promega, Madison, WI) assay according to the manufacturer's recommendations. The absorbance, measured at 492 nm from 96-well assay plates, is directly proportional to the number of living cells.

In situ *labeling with TUNEL method.* After 4–5 d of culture, neurons plated into 35 mm dishes were incubated in the absence or presence of 20 μM P118–135 at 37°C for 12 or 24 hr. At the end of the incubation time, cells were fixed in ice-cold 4% paraformaldehyde in PBS for 10 min and then rinsed twice with PBS and incubated for 30 min at room temperature in methanol containing 0.3% H_2O_2 to quench endogenous peroxidase activities. The *in situ* cell death detection was performed following the recommendations of the manufacturer (Boehringer Mannheim) and then revealed using the DAB substrate kit (Vector). Cells were stained with eosin, coverslipped with glycerol, and processed for detailed examination by light microscopy.

DNA fragmentation analysis. Neurons treated with 20 μM of P118–135 for 12 and 24 hr at 37°C were rinsed twice with PBS and then scraped off in 1 ml of lysis buffer (10 mM Tris, pH 7.4, 5 mM EDTA, 1% SDS). Proteins were digested with 200 μg/ml proteinase K in lysis buffer for 2 hr at 55°C. Neuronal DNA was extracted with phenol-chloroform, and the aqueous phase was incubated with DNase-free RNase A (100 μg/ml) and then precipitated in a solution of 0.3 M sodium acetate in ethanol overnight at −20°C. Precipitated DNA samples were resuspended in distilled water, and the DNA concentration was determined by measuring the absorbance at 260 nm. Samples of 10 μg of DNA were electrophoresed through 1.2% agarose gel containing 1 μg/ml ethidium bromide. DNA bands were visualized by UV light-transilluminator and photographed.

Measurement of caspase-like proteolytic activities. Caspase activities were measured by means of the cleavage of the substrates DEVD-pNA, YVAD-pNa, LEHD-AMC, and IEPD-AMC (Bachem). Briefly, after the indicated times of peptide treatment, cells were rinsed three times with ice-cold PBS and incubated for 20 min on ice in a 25 mM HEPES buffer,

pH 7.5, containing 1% (v/v) Triton X-100, 5 mM EDTA, 1 mM EGTA, 5 mM MgCl2, 5 mM dithiothreitol, 1 mM phenylmethylsulfonyl fluoride, 10 μg/ml each of pepstatin and leupeptine, and 5 μg/ml aprotinin. The lysate was centrifuged for 15 min at 12,000 rpm and assayed for protein by the Bradford method (Bio-Rad, Hercules, CA). Fifty micrograms of protein were incubated for 2 hr with 100 μM caspase substrate initially dissolved in DMSO. The cleavage of caspase substrates was monitored by absorbance measurements at 405 nm for DEVD-pNA and YVAD-pNa, and by fluorescence emission at 460 nm after excitation at 360 nm for LEHD-AMC and IEPD-AMC, using a Fluostar reader plate (BMG-Labtechnologies).

Results

In vivo cytotoxicity of the soluble P118–135

The *in vivo* cytotoxicity of the prion protein fragment P118–135 was estimated by measuring the electrical activity of peptide- or vehicle-treated retinas of both wild-type and $PrP^{0/0}$ mice. The electrical activity was monitored by recording the ERGs 1 and 7 d after intravitreal inoculation. Figure 1 shows the effect of peptide injections on the ERG of $PrP^{0/0}$ and wild-type mice as measured by the variation of the b-wave amplitudes. When compared with the vehicle-treated group, the P118–135-treated group exhibited significant deficits in b-wave amplitudes, direct evidence of persistent and long-term damages to retinal function. The b-wave amplitude markedly decreased at day 1 and day 7 after injection in a dose-dependent manner. The maximal decrease of b-wave amplitude was observed with the highest concentration of P118–135 and reached up to 70% of the control value. Unlike the b-wave, the a-wave amplitude was not modified significantly even 7 d after injection of P118–135 (data not shown). Interestingly, $PrP^{0/0}$ mice were sensitive to intravitreal injection of nonfibrillar P118–135 (Fig. 1). Modifications of b-wave recorded in $PrP^{0/0}$ mice follow kinetics similar to those observed with wild-type mice, suggesting strongly that the *in vivo* cytotoxicity induced by P118–135 does not require the presence of PrP-sen.

The peptide P118–135θ presents the same amino acid composition as the P118–135 peptide, but two amino acid residues are permutated at positions 120 and 131 (see Materials and Methods). It has been determined previously that this nonfusogenic fragment displays no neurotoxicity *in vitro* (Pillot et al., 2000). Accordingly, no significant decrease on the b-wave amplitudes could be observed after injection of the control peptide P118–135θ (Fig. 1).

Histology studies performed on slides from control and peptide-treated retinas 7 d after administration confirm the dramatic damages caused by the nonfibrillar P118–135 on retinal cells (Fig. 2*A*). All of the retinal changes observed occurred relatively close to the injection point, indicating a weak diffusion of the peptide. Figure 2*B* shows representative photomicrographs of PBS-treated or P118–135-treated retina sections processed through the TUNEL labeling assay. One day after intravitreal injections of P118–135 (0.3 nmol), TUNEL-positive cells were observed in the inner and outer nuclear layers as well as in the ganglion cells layer (Fig. 2*B*). No significant differences in TUNEL-labeling patterns were observed when injections were made into eyes of $PrP^{0/0}$ and wild-type mice.

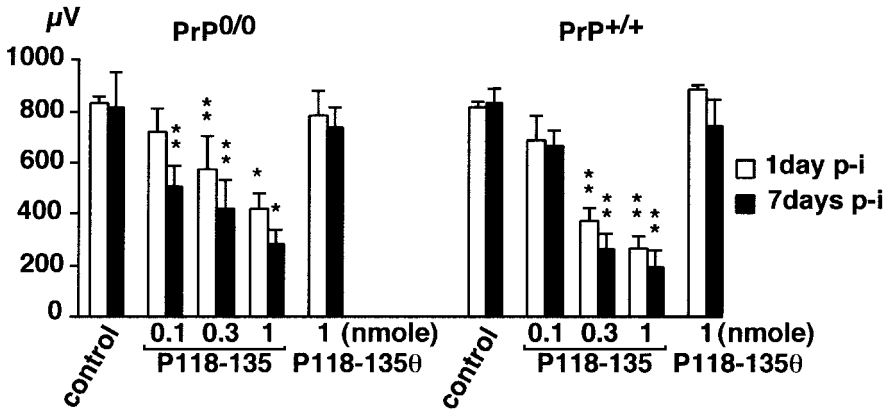

Figure 1. Alteration of the electroretinogram recording of both $PrP^{0/0}$ and wild-type mice induced by intraocular injection of the prion fragment P118–135. ERGs were recorded on overnight dark-adapted mice 1 d (*white bar*) and 7 d (*black bar*) after intravitreal inoculations of 1 μl of PBS, P118–135, and P118–135θ at the indicated quantities. The b-wave amplitudes were expressed in microvolts and were the averaged responses of two white flashes delivered 2 min apart. Histograms show the mean ± SEM of two independent experiments ($n = 2$) in which each group represents three mice injected unilaterally. Statistical significance of the difference between the means of PBS-treated and peptide-treated animals: $*p < 0.001$ and $**p < 0.05$, respectively, in an unpaired *t* test.

Intact retinas (data not shown) and retinas inoculated with PBS alone (Fig. 2*B*, *control*) showed only occasional TUNEL-positive cells.

In vitro cytotoxicity of P118–135 on primary cultured neurons

We established neuronal cultures from both $PrP^{0/0}$ and wild-type mice at E14. Under basal conditions, growth and survival of primary neuronal cultures from $PrP^{0/0}$ mice did not differ significantly from $PrP^{+/+}$ neurons, up to 8 d in serum-free N2-supplemented medium (Fig. 3).

Primary cultured neurons from $PrP^{0/0}$ and wild-type mice were exposed to 20 μM P118–135 for 72 hr. Representative phase-contrast photomicrographs show the dramatic effects induced on cortical neurons by freshly prepared P118–135 (Fig. 3). P118–135 treatment resulted in a massive breakdown and disappearance of neuronal processes and formation of shrunken cell bodies (Fig. 3). These morphological changes were also observed in neurons from $PrP^{0/0}$ mice, indicating that PrP-sen is not required for the neurotoxic effects induced by the P118–135 peptide. By contrast, incubation of neurons in the presence of the mutant peptide P118–135θ under identical experimental conditions had no effect on neuronal morphology (data not shown).

Neuronal viability was further monitored by measuring the reduction of the mitochondrial activity using the MTS assay. Nonfibrillar P118–135 treatment induces a time- and concentration-dependent decrease of the number of viable neurons for both $PrP^{0/0}$ and $PrP^{+/+}$ mice (Fig. 4, *A* and *B*, respectively). The neurotoxicity of 20 μM nonfibrillar P118–135 was statistically significant after a 12 hr incubation time and increased up to 72 hr. Moreover, neurotoxic effects were statistically significant after a 5 μM P118–135 exposure for 48 hr (Fig. 4*B*). In agreement with our morphological observations, similar kinetics and dose–response were observed when neurons from $PrP^{0/0}$ mice were incubated under the same experimental condition (Fig. 4*A*,*B*). By contrast, the nonfusogenic P118–135θ fragment was not toxic to either type of neurons even at a high concentration (40 μM) (Fig. 4*C*). We also demonstrate that the 3-d-aged (i.e., aggregated) prion synthetic peptide P106–126 was able to kill wild-type neurons but failed to kill $PrP^{0/0}$ neurons (Fig. 4*C*).

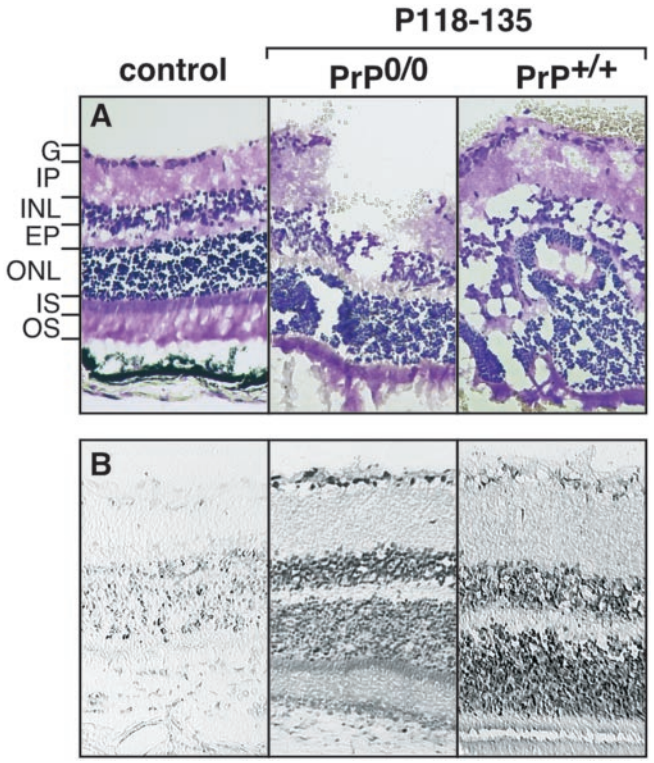

Figure 2. Effect of the PrP fragment P118–135 on retinal cell death. *A*, Representative microphotographs showing retina sections from $PrP^{0/0}$ and wild-type ($PrP^{+/+}$) mice 7 d after intraocular injections of 1 μl of PBS (*control*) or P118–135 (1 nmol). Sections were stained with 1% cresyl violet. *B*, TUNEL labeling of untreated and peptide-treated retina sections. $PrP^{0/0}$ and wild-type mice were intravitreally injected with 1 μl of PBS alone (control) or containing 0.3 nmol of freshly prepared PrP fragment P118–135. Mice eyes were enucleated 24 hr after injection, fixed, and cut on a cryostat. Retinal sections (10 μm) were processed through the TUNEL-labeling protocol and revealed with the DAB substrate kit. The nuclei of TUNEL-positive cells are *black*. Magnification, 10×. *G*, Ganglion cell; *IP*, internal plexiform; *INL*, inner nuclear layer; *EP*, external plexiform; *ONL*, outer nuclear layer; *IS*, inner segments of rods; *OS*, outer segments of rods and cones.

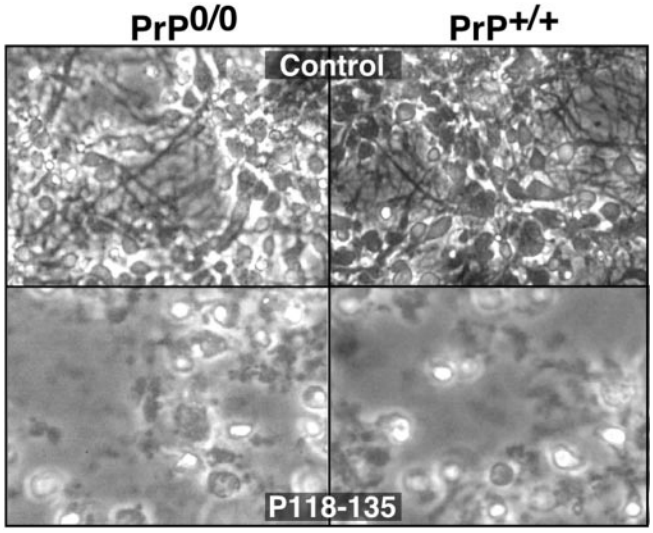

Figure 3. Neurotoxic effects of the nonfibrillar PrP fragment P118–135 on primary cultures of $PrP^{0/0}$ and wild-type neurons. Phase-contrast micrographs of representative microscopic fields are shown. Primary cultures of neurons from $PrP^{0/0}$ and wild-type mice were incubated in the absence (*Control*) or presence of 20 μM P118–135 for 48 hr at 37°C. Magnification, 25×.

Nonfibrillar P118–135 induces apoptosis to cortical neurons

To further characterize the cell death mechanisms induced by the peptide P118–135, PBS- and peptide-treated cultures of neurons were processed through the TUNEL-labeling assay (Fig. 5). After 12 hr exposure in the presence of 20 μM nonfibrillar P118–135, TUNEL-positive neurons were observed in both wild-type and $PrP^{0/0}$ neurons. The number of TUNEL-positive neurons increases after P118–135 peptide exposure, suggesting that cell death induced by the soluble P118–135 proceeds through apoptosis. $PrP^{0/0}$ and wild-type cortical neurons exposed to 20 μM soluble P118–135 for 12 hr exhibited ~16.5 and ~15% TUNEL-positive cells, respectively. The number of apoptotic cells reached ~32.6 and ~28.9% after 24 hr incubation time for both $PrP^{0/0}$ and $PrP^{+/+}$ cultured neurons, respectively (Fig. 5*B*). Neurons treated with PBS alone (Fig. 5, *control*) or with the nonfusogenic peptide P118–135θ (data not shown) showed only occasional TUNEL-positive cells.

To discriminate definitively between necrotic and apoptotic cell death pathways, the laddering of neuronal DNA was investigated. Cultured neurons from $PrP^{+/+}$ and $PrP^{0/0}$ mice were incubated for 12 and 24 hr with PBS alone or with 20 μM nonfibrillar P118–135. Peptide-treated neurons from both types of mice showed a ladder pattern of DNA degradation with bands corresponding to multiples of 180–200 base pairs (Fig. 6), whereas no DNA degradation was observed either in PBS-treated neurons (Fig. 6, *cont*) or in neurons treated with the nonfusogenic peptide P118–135θ (data not shown). DNA laddering was clearly but slightly noticeable after a 6 hr incubation time (data not shown) and was more intense after 12 and 24 hr. These experiments demonstrate clearly that soluble P118–135 exerts its neurotoxic effects via an apoptotic cell death pathway.

We demonstrated previously that P118–135 forms amyloid fibrils *in vitro* (Pillot et al., 1997). To compare the neurotoxicity of the P118–135 soluble and fibrillar forms, we incubated the P118–135 peptide for 3 d at room temperature. Cortical neurons from $PrP^{0/0}$ and $PrP^{+/+}$ mice were then incubated in the presence of soluble or fibrillar 20 μM P118–135 for 72 hr. Both treatments induced a similar increase in the number of TUNEL-positive cells, strongly suggesting that the fibrillar P118–135 peptide might also damage cortical neurons from $PrP^{0/0}$ and $PrP^{+/+}$ mice (data not shown).

Caspase activation is required for nonfibrillar P118–135-induced cell death

It was of interest to determine whether caspase activation is involved in the P118–135 neurotoxicity. Therefore, neurons from wild-type and $PrP^{0/0}$ mice were exposed independently to P118–135 for various incubation times before measurement of caspase-like activities. Exposure of cortical neurons to 20 μM nonfibrillar peptide P118–135 resulted in a time-dependent increase of the amount of caspase-3-like DEVD-pNa and caspase-9-like LEHD-AMC cleavage activities (Fig. 7). Both enzymatic activities were stimulated as early as 6 hr after treatment with 20 μM P118–135 on $PrP^{+/+}$ and $PrP^{0/0}$ cultured cortical neurons. By contrast, neither caspase-1-like YVAD-pNA nor caspase-8-like IEPD-AMC activities were augmented significantly in wild-type and $PrP^{0/0}$ neuronal extracts treated with P118–135 (Fig. 7). No significant differences of cleavage activities were observed between untreated or PBS-treated $PrP^{+/+}$ and $PrP^{0/0}$ neurons for up to 24 hr. Interestingly, the maximum level of both P118–135-stimulated caspase-3 and -9 activities was reached earlier on $PrP^{0/0}$ neurons (6 hr) compared with wild-type neurons (15 hr) (Fig. 7).

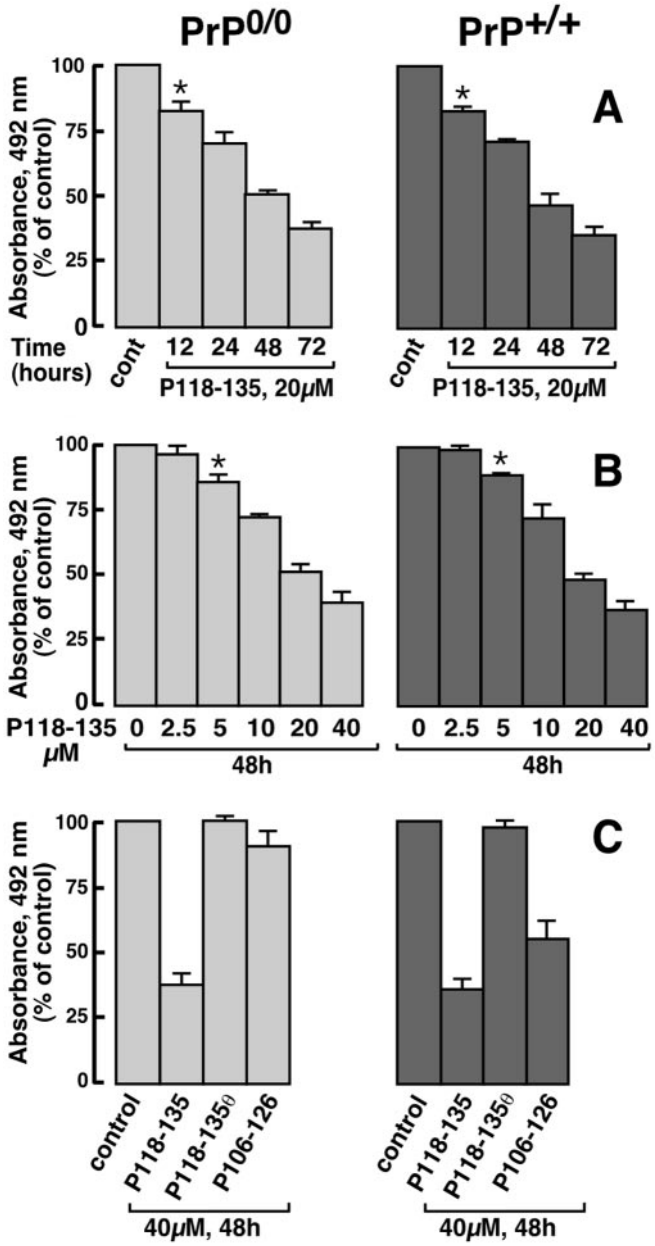

Figure 4. Neurotoxic effect of P118–135 on primary cultures of PrP$^{0/0}$ and wild-type neurons. *A*, Neurotoxicity was quantified as a function of time by the MTS assay in primary cultures of neurons from PrP$^{0/0}$ (*light gray*) and wild-type (*dark gray*) mice. *B*, Dose–response effect of the toxicity induced by the prion peptide P118–135. Neurons from PrP$^{0/0}$ (*light gray*) and wild-type (*dark gray*) mice were chronically exposed to the indicated concentrations of the PrP fragment P118–135 for 48 hr at 37°C. *C*, Specificity of the neurotoxic effect of synthetic prion fragments. Cultured PrP$^{0/0}$ and PrP$^{+/+}$ neurons were treated as indicated before being processed through the MTS assay as described in Materials and Methods. The data are means ± SEM of four independent experiments with three determinations. Statistically significant differences between control and peptide-treated groups: $*p < 0.01$ versus control; Student's *t* test.

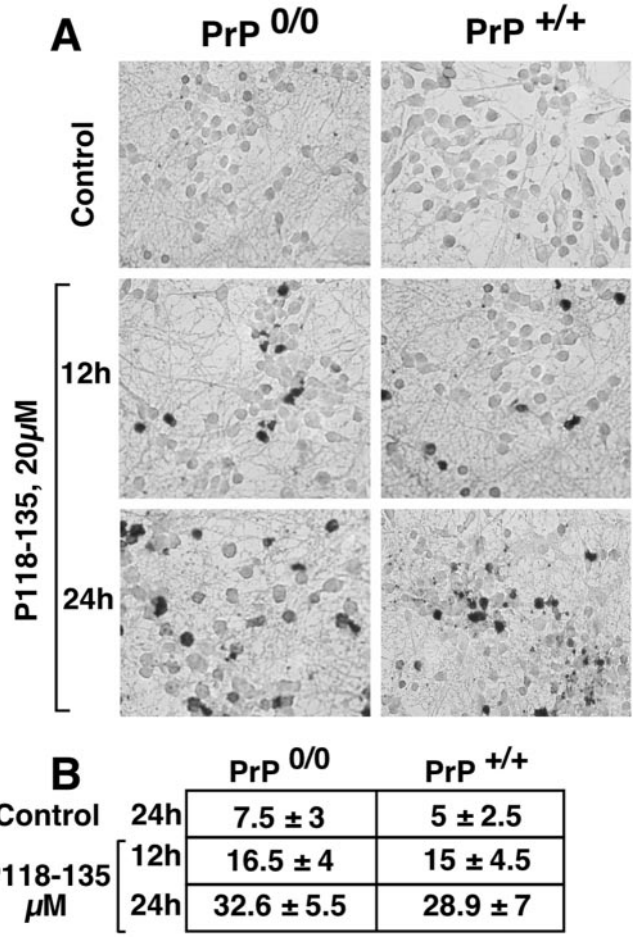

Figure 5. P118–135-induced neuronal death monitored by the *in situ* TUNEL-labeling method. *A*, Cortical PrP$^{0/0}$ and PrP$^{+/+}$ neurons were cultured in the absence (*Control*) or presence of 20 μM P118–135 for 12 or 24 hr at 37°C. At the end of the incubation time, neurons were rinsed, fixed with paraformaldehyde, and processed through the TUNEL-labeling method according to the manufacturer's recommendations. The TUNEL-positive cells were revealed with the DAB substrate kit and appear in *black*. Nonreactive cells were stained with eosin and appear in *light gray*. *B*, Quantitative determination of TUNEL-positive neurons. The percentage of TUNEL-positive cells was obtained by counting 10 independent microscopic fields (~70 cells) in three separate experiments. Results are expressed as the percentage of TUNEL-positive cells and are means ± SEM ($n = 3$).

Discussion

In the present paper, we demonstrate for the first time the following: (1) in a nonfibrillar conformation, the membrane-destabilizing P118–135 prion peptide exhibits *in vivo* cytotoxicity at micromolar concentrations; (2) after peptide exposure, cell death proceeds through an apoptotic pathway involving early caspase-3 and -9 activation; and (3) the presence of PrP-sen is not an obligatory requirement for nonfibrillar P118–135 prion peptide-induced neurotoxicity.

The retina is a well suited model to study the molecular events leading to cell death during the course of neurodegenerative diseases (Jen et al., 1998; Ettaiche et al., 2000). First, retina is an integral part of the CNS that is poorly provided with proteolytic activities; second, the diffusion of injected peptides is limited because eyes are closed systems; and third, retina is susceptible to infection and disease caused by prions (Fraser, 1982, 1996). Finally, the electroretinogram recording analysis provides a direct monitoring of the physiological activity of retina and accurately reflects the integrity of retinal neurons. Thus, taking advantage of the fact that transgenic and PrP$^{0/0}$ mice are available, we have adapted the technique of intravitreal peptide injection, usually done in rat and hamster eyes, to the mouse.

Direct intravitreal injections of the nonfibrillar P118–135 peptide result in an important reduction of the electrical activity of the retina, likely by inducing retinal cell death. Because no recovery of the electroretinogram recordings was observed 7 d

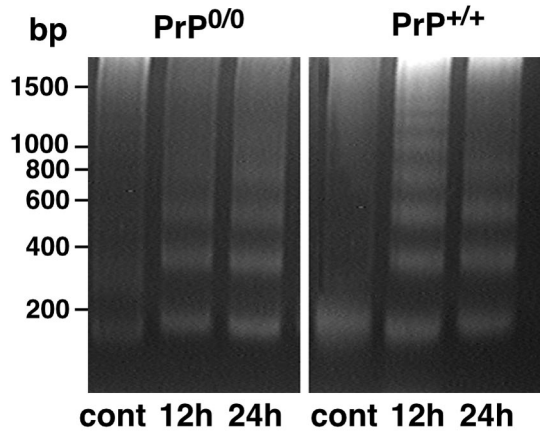

Figure 6. Induction of the neuronal DNA fragmentation by the PrP peptide P118–135. Cortical neurons from both PrP $^{0/0}$ and PrP $^{+/+}$ mice were cultured in the absence (*cont*) or presence of 20 μM P118–135 for 12 and 24 hr at 37°C. At the end of the incubation time, the neuronal DNA was extracted and electrophoresed on a 1.2% gel agarose as described in Materials and Methods. DNA bands were visualized by staining with ethidium bromide. DNA size markers are indicated on the *left side* of the gel. *bp*, Base pair.

after injection, the deleterious effects of the peptide P118–135 can be considered as irreversible. Histological observations of the 7 d injected retina demonstrate clearly the dramatic injuries induced by the P118–135 peptide on the different retinal cells layers. Moreover, the positive TUNEL-labeling staining of 1 d treated retina slides suggests strongly that *in vivo* cell death induced by the nonfibrillar P118–135 is mediated through an apoptotic process. P118–135-treated mice exhibit significant deficits in b-wave amplitudes without modification of the a-wave amplitude. These results suggest that the nonfibrillar P118–135 peptide causes retinal cell death but weakly damages the photoreceptor cells. Interestingly, patients with Creutzfeldt-Jakob disease have been reported to present a selective loss of the b-wave amplitude without alteration of the a-wave amplitude (de Seze et al., 1998; Katz et al., 2000). Further experiments will be performed to precisely define the retinal cell type affected by P118–135 toxic effects. For instance, the importance of microglial cells in the neuronal death during TSE development has been underlined by several investigators (Brown and Kretzschmar, 1997; Giese et al., 1998).

To identify precisely the molecular mechanisms involved in P118–135 peptide-induced cell death, we performed some experiments on cultured mice cortical neurons. We demonstrate clearly that, *in vitro*, the apoptotic pathway triggered by the nonfibrillar P118–135 peptide involves the activation of caspases, resulting in DNA condensation and fragmentation. Indeed, the prion fragment P118–135 activates caspases-3 and –9 but fails to modulate the levels of caspases-8 and –1. These data suggest that plasma membrane death receptors mediating cell death might not be involved in this process. Moreover, caspase-9 activation induced by exposure of neurons to the soluble P118–135 peptide could reflect an alteration of the membrane of intracellular organelles.

As proposed previously (Pillot et al., 1996, 2000), it is likely that the soluble P118–135 fragment exerts its toxic properties through its capacity of tilted insertion into membranes at an angle of 40–45°. A variant peptide P118–135θ presenting a permutation of two amino acid residues compared with the P118–135 peptide exhibits no fusogenic activity (Pillot et al., 1997) and is not toxic to cultured rat cortical neurons (Pillot et al., 2000). Interestingly, we show here that the mutant peptide P118–135θ is devoid of *in vivo* toxicity on retinal cells because no alteration of the electrical activity of the retina has been measured. These results, confirmed by *in vitro* experiments, suggest strongly that the membrane destabilizing properties of the nonfibrillar P118–135 peptide also account for part of its cytotoxic effects.

Although the mechanisms involved in cell death induced by prion peptides are not understood completely, it has been shown that the neurotoxicity of the prion peptide P106–126 was dependent on its aggregation state (Forloni et al., 1993; Hope et al., 1996; Jobling et al., 1999; Salmona et al., 1999; Ettaiche et al., 2000; Rymer and Good, 2000). Indeed, solutions of peptide P106–126 having substantial β-sheet structure and amyloid content reduced neuron viability, whereas solutions lacking highly ordered structures were not toxic. By contrast, our results show that the prion fragment P118–135 in a nonfibrillar form induces cell death both *in vivo* and *in vitro*. These results are in agreement with our previous data showing that the soluble form of the P118–135 peptide induces membrane destabilization (Pillot et al., 1997). However, because we also demonstrate that the ag-

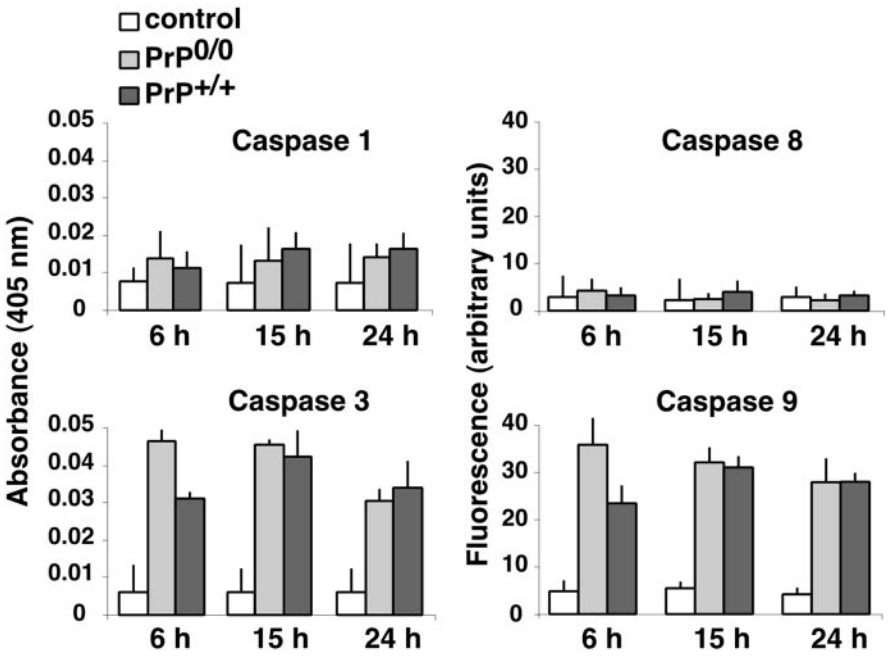

Figure 7. Modification of caspase-like activities induced by the peptide P118–135 on cortical neurons. Cortical neurons from both PrP $^{0/0}$ (*light gray histogram*) and PrP $^{+/+}$ (*dark gray histogram*) mice were cultured in the absence (*control*) or presence of 20 μM soluble P118–135 at 37°C. After the indicated incubation time, the DEDVD-pNa (caspase-3 substrate) and YVAD-pNa (caspase-1 substrate) cleavage activities in cell lysates were assayed by measuring the absorbance at 405 nm, whereas IEPD-AMC (caspase-8 substrate) and LEHD-AMC (caspase-9 substrate) cleavage activities were measured by fluorescence emission at 460 nm, as described in Materials and Methods. Because no significant differences in the caspase cleavage activities have been observed between wild-type and PrP $^{0/0}$ neurons under PBS-treated conditions up to 24 hr, the control histograms represent the means of values obtained for both types of neurons. Data are means ± SE of two independent experiments with two determinations each.

gregated form of P118–135 is toxic [Pillot et al. (2000), and this work], it seems that both fusogenic and aggregated peptides are capable of inducing neuronal cell death.

One important finding of our work is that cell death induced by the nonfibrillar P118–135 peptide does not require the expression of endogenous PrPc. Indeed, the peptide P118–135 exerts its cytotoxic effects on the retina of wild-type and $PrP^{0/0}$ mice and induces apoptosis to cortical neurons of both types of mice. By contrast, the P106–126 peptide fully exerts its toxicity on PrP-expressing neurons and fails to be toxic on PrP-devoid cells *in vitro* (Fig. 4*C*) (Brown et al., 1996). Altogether, our results point out the differences between molecular mechanisms involved in the cytotoxicity induced by the P106–126 and P118–135 prion peptides. In contrast to other prion fragments, the toxic effects of P118–135 are independent of both its aggregation state and the neuronal PrP-sen expression. This could account for the different *in vivo* neurodegeneration mechanisms occurring during the development of TSEs.

Many reports have shown that synthetic prion peptides could provide insights into understanding the molecular mechanisms involved in the pathogenesis of neurodegenerative diseases (Tagliavini et al., 2001a). In some cases, the low level of PrP-res aggregates recovered in TSE-affected brains is not easily reconcilable with the widely held belief that amyloid fibrils of PrP-res are solely responsible for neuronal cell death. In this context, a specific transmembrane isoform of PrP was found in brains of patients with GSS A117V as well as in transgenic mice expressing the A117V mutated PrP. In both cases, no protease-resistant prion fragments characterizing other TSEs were found (Hegde et al., 1998, 1999). On the basis of these observations, the authors proposed that the transmembrane isoform of PrP rather than the aggregation of PrP-res plays a crucial role in neuropathogenesis. Recently, a remarkable accumulation of PrP amyloid peptides has been isolated from GSS brain (Tagliavini et al., 2001b). Sequence analysis and mass spectrometry have shown that the main component is a 7 kDa PrP fragment, both N- and C-terminal truncated, encompassing residues ~88 to ~146 (Tagliavini et al., 2001b). Thus, it seems that under pathological situations, small PrP peptides may be produced and either remain in a soluble state or form amyloid fibrils. We showed previously that the synthetic peptide P118–135 is neurotoxic under both its nonaggregated and fibrillar conformations (Pillot et al., 2000). An alternative explanation could be the formation of toxic (either fusogenic or amyloidogenic) partial sequences of PrP from a specific isoform of the protein (^{Cterm}PrP), preferentially expressed in some TSEs.

In conclusion, we show clearly that the nonfibrillar prion fragment P118–135 induces neuronal cell death *in vivo* independently of the PrP expression. Our results pointed out the fact that fully matured isoforms of PrP with aberrant topology or some proteolytic PrP fragments produced during the development of GSS disease could insert into cell membranes and perturb their structures, thus leading to neuronal damages in the absence of PrP-res deposits.

References

Brasseur R, Pillot T, Lins L, Vandekerckhove J, Rosseneu M (1997) Peptides in membranes: tipping the balance of membrane stability. Trends Biochem Sci 22:167–171.

Brown DR, Kretzschmar HA (1997) Microglia and prion disease: a review. Histol Histopathol 12:883–892.

Brown DR, Schmidt B, Kretzschmar HA (1996) Role of microglia and host prion protein in neurotoxicity of a prion protein fragment. Nature 380:345–347.

Büeler H, Fischer M, Lang Y, Bluethmann H, Lipp H-P, DeArmond SJ, Prusiner SB, Aguet M, Weissmann C (1992) Normal development and behaviour of mice lacking the neuronal cell surface PrP protein. Nature 356:577–582.

Chabry J, Checler F, Vincent JP, Mazella J (1990) Colocalization of neurotensin receptors and of the neurotensin-degrading enzyme endopeptidase 24–16 in primary cultures of neurons. J Neurosci 10:3916–3921.

de Seze J, Hache JC, Vermersch P, Arndt CF, Maurage CA, Pasquier F, Laplanche JL, Ruchoux MM, Leys D, Destee A, Petit H (1998) Creutzfeldt-Jakob disease: neurophysiologic visual impairments. Neurology 51:962–967.

Ettaiche M, Pichot R, Vincent JP, Chabry J (2000) In vivo cytotoxicity of the prion protein fragment 106–126. J Biol Chem 275:36487–36490.

Forloni G, Angeretti N, Chiesa R, Monzani E, Salmona M, Bugiani O, Tagliavini F (1993) Neurotoxicity of a prion protein fragment. Nature 362:543–546.

Fraser H (1982) Neuronal spread of scrapie agent and targeting of lesions within the retino-tectal pathway. Nature 295:149–150.

Fraser H (1993) Diversity in the neuropathology of scrapie-like diseases in animals. Br Med Bull 49:792–809.

Fraser JR (1996) Infectivity in extraneural tissues following intraocular scrapie infection. J Gen Virol 77:2663–2668.

Giese A, Brown DR, Groschup MH, Feldmann C, Haist I, Kretzschmar HA (1998) Role of microglia in neuronal cell death in prion disease. Brain Pathol 8:449–457.

Haik S, Peyrin JM, Lins L, Rosseneu MY, Brasseur R, Langeveld JP, Tagliavini F, Deslys JP, Lasmezas C, Dormont D (2000) Neurotoxicity of the putative transmembrane domain of the prion protein. Neurobiol Dis 7:644–656.

Hay B, Barry RA, Lieberburg I, Prusiner SB, Lingappa VR (1987) Biogenesis and transmembrane orientation of the cellular isoform of the scrapie prion protein. Mol Cell Biol 7:914–920.

Hegde RS, Mastrianni JA, Scott MR, DeFea KA, Tremblay P, Torchia M, DeArmond SJ, Prusiner SB, Lingappa VR (1998) A transmembrane form of the prion protein in neurodegenerative disease. Science 279:827–834.

Hegde RS, Tremblay P, Groth D, DeArmond SJ, Prusiner SB, Lingappa VR (1999) Transmissible and genetic prion diseases share a common pathway of neurodegeneration. Nature 402:822–826.

Hope J, Shearman MS, Baxter HC, Chong A, Kelly SM, Price NC (1996) Cytotoxicity of prion protein peptide (PrP106–126) differs in mechanism from the cytotoxic activity of the Alzheimer's disease amyloid peptide, Aβ 25–35. Neurodegeneration 5:1–11.

Jen LS, Hart AJ, Jen A, Relvas JB, Gentleman SM, Garey LJ, Patel AJ (1998) Alzheimer's peptide kills cells of retina in vivo. Nature 392:140–141.

Jobling MF, Stewart LR, White AR, McLean C, Friedhuber A, Maher F, Beyreuther K, Masters CL, Barrow CJ, Collins SJ, Cappai R (1999) The hydrophobic core sequence modulates the neurotoxic and secondary structure properties of the prion peptide 106–126. J Neurochem 73:1557–1565.

Katz BJ, Warner JE, Digre KB, Creel DJ (2000) Selective loss of the electroretinogram B-wave in a patient with Creutzfeldt-Jakob disease. J Neuroophthalmol 20:116–118.

Kretzschmar HA, Stowring LE, Westaway D, Stubblebine WH, Prusiner SB, Dearmond SJ (1986) Molecular cloning of a human prion protein cDNA. DNA 5:315–324.

Locht C, Chesebro B, Race R, Keith JM (1986) Molecular cloning and complete sequence of prion protein cDNA from mouse brain infected with the scrapie agent. Proc Natl Acad Sci USA 83:6372–6376.

Lopez CD, Yost CS, Prusiner SB, Myers RM, Lingappa VR (1990) Unusual topogenic sequence directs prion protein biogenesis. Science 248:226–229.

Pillot T, Goethals M, Vanloo B, Talussot C, Brasseur R, Vandekerckhove J, Rosseneu M, Lins L (1996) Fusogenic properties of the C-terminal domain of the Alzheimer beta-amyloid peptide. J Biol Chem 271:28757–28765.

Pillot T, Lins L, Goethals M, Vanloo B, Baert J, Vandekerckhove J, Rosseneu

M, Brasseur R (1997) The 118–135 peptide of the human prion protein forms amyloid fibrils and induces liposome fusion. J Mol Biol 274:381–393.

Pillot T, Drouet B, Pincon-Raymond M, Vandekerckhove J, Rosseneu M, Chambaz J (2000) A nonfibrillar form of the fusogenic prion protein fragment [118–135] induces apoptotic cell death in rat cortical neurons. J Neurochem 75:2298–2308.

Rymer DL, Good TA (2000) The role of prion peptide structure and aggregation in toxicity and membrane binding. J Neurochem 75:2536–2545.

Salmona M, Malesani P, De Gioia L, Gorla S, Bruschi M, Molinari A, Della Vedova F, Pedrotti B, Marrari MA, Awan T, Bugiani O, Forloni G, Tagliavini F (1999) Molecular determinants of the physicochemical properties of a critical prion protein region comprising residues 106–126. Biochem J 342:207–214.

Tagliavini F, Forloni G, D'Ursi P, Bugiani O, Salmona M (2001a) Studies on peptide fragments of prion proteins. Adv Protein Chem 57:171–201.

Tagliavini F, Lievens PM, Tranchant C, Warter JM, Mohr M, Giaccone G, Perini F, Rossi G, Salmona M, Piccardo P, Ghetti B, Beavis RC, Bugiani O, Frangione B, Prelli F (2001b) A 7-kDa prion protein (PrP) fragment, an integral component of the PrP region required for infectivity, is the major amyloid protein in Gerstmann-Straussler-Scheinker disease A117V. J Biol Chem 276:6009–6015.